科学通报 2018 年 第 63 卷 第 23 期: 2335 ~ 2347
评 述
《中国科学》杂志社
SCIENCE CHINA PRESS

三维细微观结构的折叠和组装方法

范智超, 张帆, 张一慧*

清华大学航天航空学院工程力学系, 教育部应用力学重点实验室, 北京 100084
* 联系人, E-mail: yihuizhang@tsinghua.edu.cn

2018-04-23 收稿, 2018-06-10 修回, 2018-06-12 接受, 2018-07-19 网络版发表
国家自然科学基金(11672152, 11722217)和组织部“青年千人计划”资助

摘要 近年来, 尺度介于几十纳米到几百微米之间的三维(3D)细微观结构受到研究人员越来越多的关注. 其原因在于, 通过在先进材料中形成具有特定几何拓扑的三维细微构造, 可以使得宏观材料在声、光、热、力、电学等方面表现出新的特性. 这种具备天然材料中不存在的超常物理特性的材料也被称为“超材料”. 由于超材料在各类微系统技术中的巨大应用前景, 三维细微观结构的设计与制备方法日益成为国内外的研究热点. 目前除了3D打印这类较成熟的增材制造方法之外, 应力控制的折叠方法和力学引导的组装方法也相继被提出, 并因其在材料类型、几何拓扑、尺度范围等方面的优势, 亦逐渐成为研究焦点. 本文综述了这两类方法的最新进展, 并对其设计原理、成形过程以及相关的理论和应用进行分析和总结.

关键词 三维组装, 4D 打印, 三维细微观结构, 压缩屈曲

在先进材料(如单晶硅、石墨烯等)中形成具有特定几何拓扑的三维细微观结构, 可以让材料在宏观表现出全新的物理性质(如负折射率[1]和人造磁性[2]等). 因为这些性质往往在天然材料中不存在, 所以这类材料有时也被称为“超材料”[1~5]. 由于超材料的性质高度依赖于细微观的三维几何构造, 因此三维细微观结构的设计与制备日益成为科学研究的热点.

早期的“超材料”领域研究多集中于光学超材料. 例如, 通过形成具有亚波长特征尺度的三维细微观周期结构, 可以精确地控制电磁波(如微波[1,6~8]、太赫兹波[9~11]、红外光波和可见光波[12~16])的传播. 这些电磁波的波长范围通常在几十纳米到几毫米之间, 而制备具有相应特征尺度的三维结构对于传统的微加工工艺是很有挑战的, 因此需要在材料科学和制造工艺方面有所突破. 以光子超材料为例, 目前三维细微观结构的制备方法主要有胶体自组装[17]、全息光刻[18~21]、直接半导体生长和逐层生长[22~25]以及双光子或多光子光刻[26~29]. 在这些方法中, 通常需要先使用特定材料形成所需要的三维构型, 然后通过沉积或生长的方式将材料转换为具有所需光学性质的材料.

随着近些年科学技术的进步, “超材料”的发展已经和更多种类的物理性质关联起来, 除了光学性质[12~16]之外, 还体现在热学[30~32]、声学[33~36]、力学[37~45]和电磁学[1,6~8]等方面. 例如, 最近的研究表明, 陶瓷和金属微纳米晶格形式的超材料[37,40,42]可以实现常规材料不具有的超高比强度和比刚度. 随着多光子成形技术和大面积投影微立体平版印刷术(LAPμSL)[38]的出现, 具有不同尺度范围(从纳米到厘米)三维细微观结构的超材料得到了很大的发展. 例如, 利用多材料投影微立体平面印刷方法(PμSL), 研究者设计出具有不同热扩散系数的三维周期点阵单元, 实现了具有可调三维负热膨胀系数的轻质超材料[46]; 利用具有强大的低频Mie共振[47~49]特性的三

引用格式: 范智超, 张帆, 张一慧. 三维细微观结构的折叠和组装方法. 科学通报, 2018, 63: 2335–2347
Fan Z C, Zhang F, Zhang Y H. Folding and assembly methods for forming three-dimensional mesostructures (in Chinese). Chin Sci Bull, 2018, 63: 2335–2347, doi: 10.1360/N972018-00396

维结构可形成软声学超材料; 利用微流体方法产生随机分散在凝胶基质中的大孔硅酮微珠, 可以实现宏观材料在较宽的频率范围内具有负的声学相速度[48].

三维细微观结构也为微系统技术的工程设计提供了更多的选择, 其应用领域包括生物医学器件[50~54]、微机电系统(MEMS)[55~57]、能量存储平台[58~63]、光电子器件[64,65]、电子器件[66~73]等等. 目前在这些领域中, 器件还是以传统的平面结构为主, 若能采用具有三维细微观结构的先进材料, 其效率和性能有望得到显著提高[67]. 三维细微观结构的设计与制备方法正得到广泛的研究, 除了前面介绍的光学技术之外, 3D打印这类增材制造技术[73~83]也有了显著的发展. 近期, 应力控制的折叠方法和力学引导的组装方法相继得到报道. 与其他方法相比, 这两类方法的优势是它们与传统平面微电子加工工艺和薄膜沉积技术相兼容, 可充分利用传统二维微加工技术的优点, 制备出复杂的三维细微观结构.

本文重点介绍应力控制的折叠方法和力学引导的组装方法的最新成果, 阐述基于折叠和力学组装的设计和制备原理, 总结和分析了相关理论和应用, 并展望了未来的挑战和机会.

1 应力控制的折叠方法

应力控制的折叠方法充分利用了传统平面微纳米加工工艺, 包括半导体和集成电子行业常用的光刻、薄膜沉积、材料生长(包括外延生长、掺杂)等先进技术, 通过引入材料的内应力, 诱发平面结构的弯曲折叠变形, 得到具有复杂构型的三维细微观结构. 这类方法主要有4D打印和微纳折纸, 接下来进行详细介绍.

1.1 4D打印

在本方法中, 首先利用3D打印技术制备出双层或多层平面结构, 其中每一层的材料属性不相同, 然后利用外部刺激(如水浸润, 加热), 使得结构内部产生应变失配, 诱导其发生自折叠或自弯曲, 进而变形得到所需的三维构型, 而这些三维构型通常很难通过3D打印方法直接得到. 4D打印方法要求所使用的材料对外部刺激有明显的变形响应, 其中比较有代表性的材料有水凝胶[84~86]和形状记忆聚合物(SMP)[87~89].

图1(a)展示了基于水凝胶材料的4D打印技术流程, 其中初始双层平面结构由3D打印技术使用水凝胶复合材料墨水[86]打印制备得到, 图中的纤维方向决定了每层材料的各向异性刚度和溶胀行为. 在外部刺激下, 由于双层结构中的顶层和底层之间的不同溶胀变形, 整体结构发生折叠变形, 进而实现了结构在空间内变化的曲率分布. 结构的最终构型主要取决于材料的弹性模量、溶胀比、两层的厚度比和总厚度. 通过对铁摩辛柯建立的双层金属条带模型进行扩展, 可以建立定量的理论模型, 预测在这些因素综合影响下初始双层结构的最终变形. 此外, 通过外部刺激(如加热)还可以实现三维构型的逆变形[86], 使之回复到初始平面状态. 将水凝胶与惰性高分子材料层合在一起, 还可以形成暴露于水[84,85]时能够折叠、卷曲、扭曲和线性膨胀或收缩的自变形结构. 在图1(c)中展示了一组基于水凝胶的4D打印方法得到的复杂花状结构[86].

在基于SMP的4D打印技术中, 初始双层结构由一层纯基体和一层嵌入了SMP纤维的基体薄板组成(如图1(b)所示), 其中SMP的玻璃化转变温度为T_g. 首先在高温T_h(T_h>T_g)下对初始结构进行拉伸, 然后在低温T_l(T_l<T_g)下冷却并释放外部施加的力, 此时基体材料倾向于回复到初始状态, 而SMP则倾向于保持变形后的状态, 由此引起的结构内部应变失配使得整体结构产生变形, 从而得到最终的三维构型. 值得说明的是, 当温度再次升到T_h, 结构将回复到二维初始状态. 在图1(d)中展示了通过本方法得到的一些三维结构[88]. 此外, 若对基体材料和SMP进行有针对性地设计和选择, 本方法在未来还有望实现结构以特定的速度对外部刺激进行响应.

1.2 微纳折纸

折叠变形是微纳尺度下折纸设计的基础[69,90~93], 在前人的研究中, 其所需的驱动力多源于毛细力、薄膜残余应力和主动材料对外界刺激的响应. 图2(a)展示了利用毛细作用力[94~99]驱动薄板折叠变形的流程: 首先将焊料加热到其熔点以上, 此时焊料融化变形为表面能最小的类圆柱形结构, 驱动下方薄板发生折叠变形, 最后通过冷却让焊料重新固化. 有一些研究利用水滴的毛细力实现薄膜的折叠变形[100,101]. 基于毛细力的驱动策略多用来实现各种封闭形式的多面体细微观结构[97,99,100], 如图2(b)所示[99].

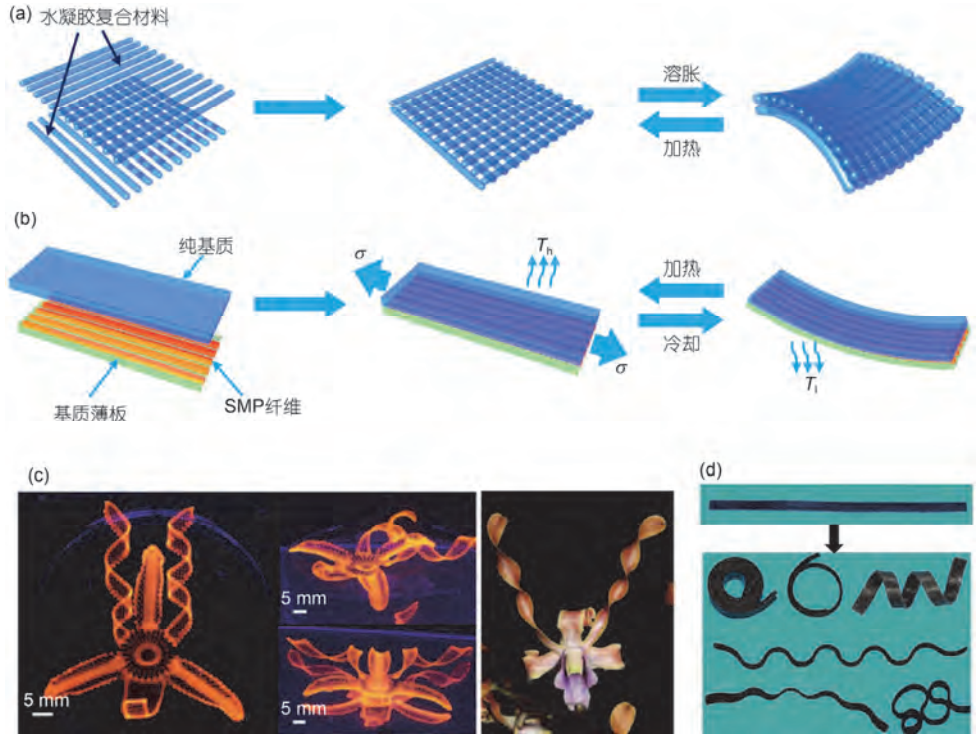

图 1 (网络版彩色)4D打印方法的基本原理示意图和对应的实例. (a) 利用水凝胶材料的 4D打印基本流程; (b) 利用SMP材料的 4D打印基本流程; (c) 利用水凝胶材料折叠变形得到的花状三维结构[86]; (d) 利用SMP材料折叠变形得到的典型结构[88]

Figure 1 (Color online) 4D printing schemes and representative structures. (a) Schematic illustrations of 4D printing using hydrogel; (b) schematic illustrations of 4D printing using SMP; (c) a flower-like structure formed by folding of hydrogel[86]; (d) some representative structures formed by folding of SMP[88]

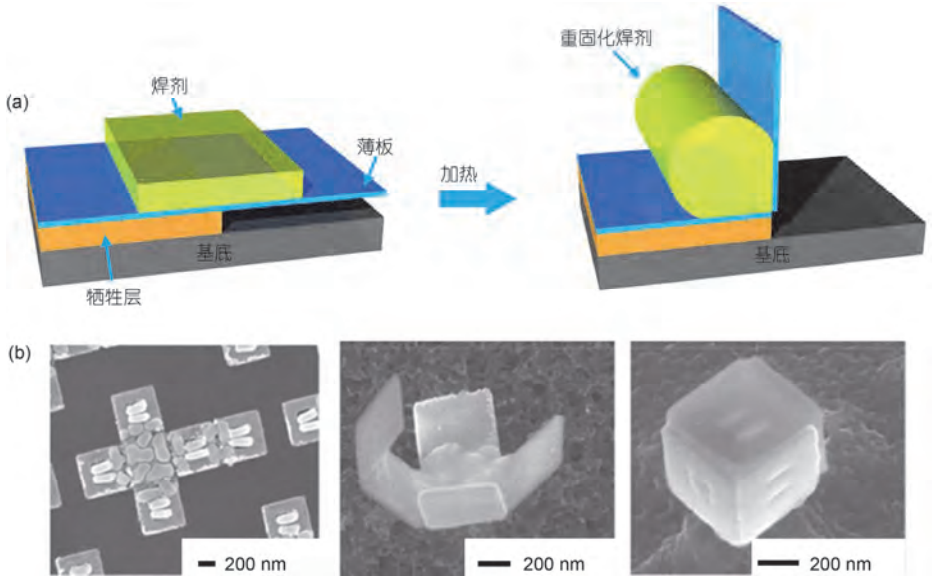

图 2 (网络版彩色)毛细力驱动折叠变形的基本原理示意图(a)和典型结构(b)[99]

Figure 2 (Color online) Schematic illustration (a) and representative structures (b) of capillary-driven folding[99]

基于薄膜残余应力的方法常依赖于多层结构中不同材料之间的应变失配, 如图3(a)所示, 当去除下面的牺牲层[102~104]时引发上层有预应力的纳米薄膜发生卷曲变形. 多层结构中沿厚度方向的应变梯度

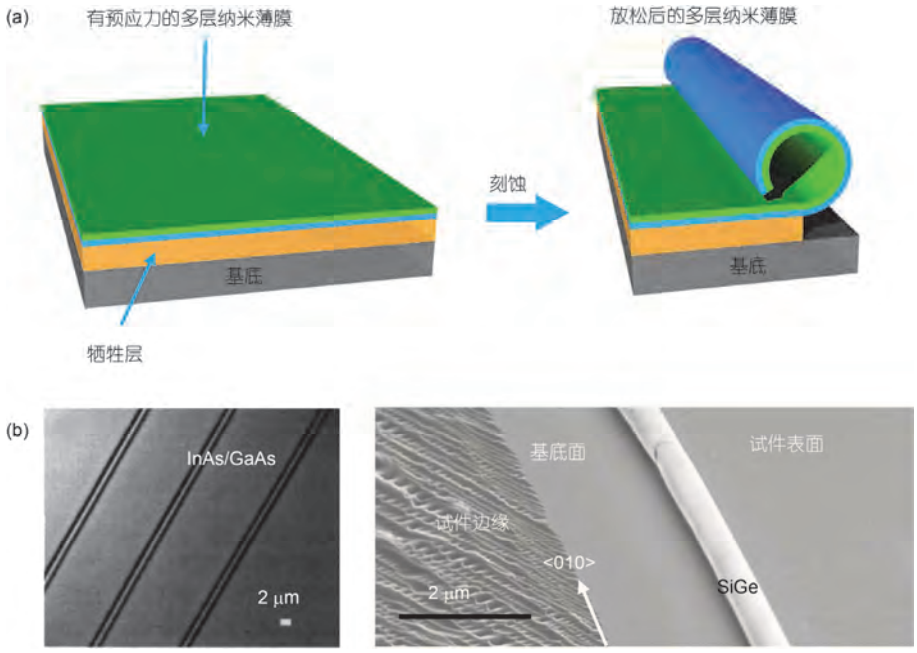

图 3 (网络版彩色)薄膜残余应力驱动折叠变形的基本原理示意图(a)和典型结构(b)[103]

Figure 3 (Color online) Schematic illustration (a) and representative structures (b) of thin-film residual stress-driven folding[103]

可通过调整薄膜沉积工艺中的相关参数(如温度、频率、成分和沉积速率)来控制. 这种策略可以在多种材料体系(如Pt, ZnO, Al_2O_3, Si_xN_y, TiO_2, SiGe, Si_xN_y-Ag, InGaAs-GaAs和Pd-Fe-Pd)中产生具有管状、涡卷状和多面体状几何构型的细微观结构[70~72,102,103,105~113]. 在图3(b)展示了利用该方法实现的一些管状结构[103].

另一种策略则利用主动材料(如: 水凝胶[114~119], SMP或形状记忆合金(SMA)[120~122], 液晶弹性体[123,124]和光敏聚合物[125,126])对外部刺激的响应, 使结构产生面内或面外(即厚度方向)的非均匀应变, 进而变形为所期望的三维构型. 如图4(a)所示, 以含有水凝胶夹层的多层结构为例, 利用水凝胶的溶胀行为在多层结构中引入应变失配, 进而灵活地控制平面结构的三维变形. 在图4(b)中展示了几种利用该策略得到的复杂三维模型[119].

在上述微纳折纸方法中, 结构最终的三维构型是由系统总能量最小化确定的平衡状态. 系统总能量通常包括结构应变能(即各层薄膜的弯曲能量和拉伸/压缩能量)和外力势, 通过建立相应的力学模型可以分析各种驱动力、结构几何参数和最终三维构型之间的依赖关系. 这些方法与现有的平面微加工工艺相兼容, 有潜力制备出具有实用价值的新型微纳器件, 如3D电子器件、光学器件和生物医学器件等. 目前已有一些新型微器件得到报道, 如: 对捕光效率有提升的太阳能电池[101], 能够分离和隔离单个细胞的细胞夹持器[110], 可使用标准医用注射器植入的微天线[111], 可用于射频集成电路的微电感[66,127]等.

在微纳米尺度实现结构的可逆和可编程自折叠三维变仍具有挑战性, 特别在活性材料(如SMP/SMA)的二维微纳薄膜成形以及与高性能电子材料的异质集成方面还有很大的发展空间. 在最近的报道中, 研究者使用石墨烯薄膜作为结构材料[128,129], 由于其厚度为原子量级, 使得在结构中实现极小的曲率半径成为可能. 通过面内或面外加载, 具有剪纸结构且横向特征尺寸为2 μm的石墨烯薄膜被组装为三维构型[128]. 利用热驱动可实现石墨烯薄膜从衬底上自发撕开或剥离[129]. 在这些例子中, 采用磁力或其他外部刺激成功将先进材料组装为三维结构, 为先进材料的折纸设计提供了参考, 同时原子模拟技术则从底层物理层面揭示了薄膜的变形机理[130~135].

2 力学引导的组装方法

前述应力控制的折叠方法多适用于制备几何构型较简单的弯曲结构(例如管状或卷轴状)、闭合或开放的多面体结构和圆柱形结构. 近期发展起来的基于力学引导的组装方法提供了一种设计制备三维细

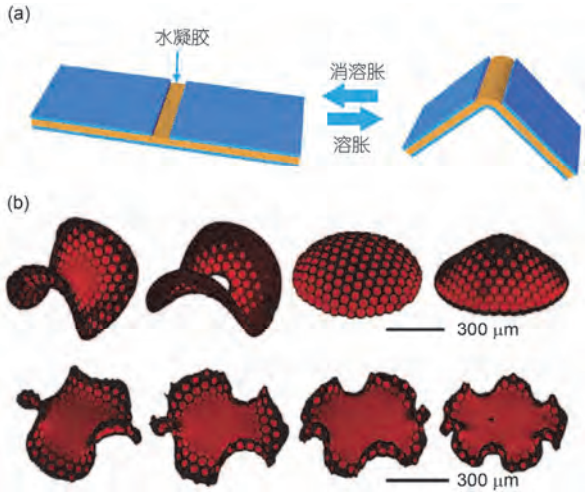

图 4 (网络版彩色)利用主动材料对外部刺激的响应来驱动折叠变形的基本原理示意图(a)和典型结构(b)[119]

Figure 4 (Color online) Schematic illustration (a) and representative structures (b) of folding method that relies on the stimuli response of active materials[119]

微观结构的新途径，该方法能精确地控制从初始平面结构到三维结构的变形过程[68]，可以得到具有更多几何拓扑类型的三维构型，同时保持了与前述应力控制的折叠方法以及传统平面加工工艺的兼容性.

本方法的基本流程如图5(a)所示. 首先利用传统平面微加工技术制备出预先设计的初始二维结构，然后将之与预拉伸的弹性基底建立选择性的黏接[67,68,136,137]，最后通过释放基底，引起黏接区域的收缩，进而使得二维结构发生面外屈曲，变形为三维结构. 该方法的关键控制变量包括：初始二维结构的几何设计，材料的力学特性，黏接区域的位置以及基底预拉伸应变的大小. 通过建立定量的力学模型可以高精度地揭示这些控制变量对结构变形的影响，调整这些参数能得到各式各样形状复杂的三维结构[67,68,136~138].

在力学模型的指导下，该方法可以组装得到的几何拓扑类别非常广泛，包括三维螺旋、类球形筐、长方体框、星形框架、花形框架等各种由单条带和/或多条带组成的三维结构[68]和各类形状复杂的曲面状三维结构[136,137,139]. 在图5(b)中展示出了部分利用半导体单晶硅材料组装得到的精细条带状三维微观

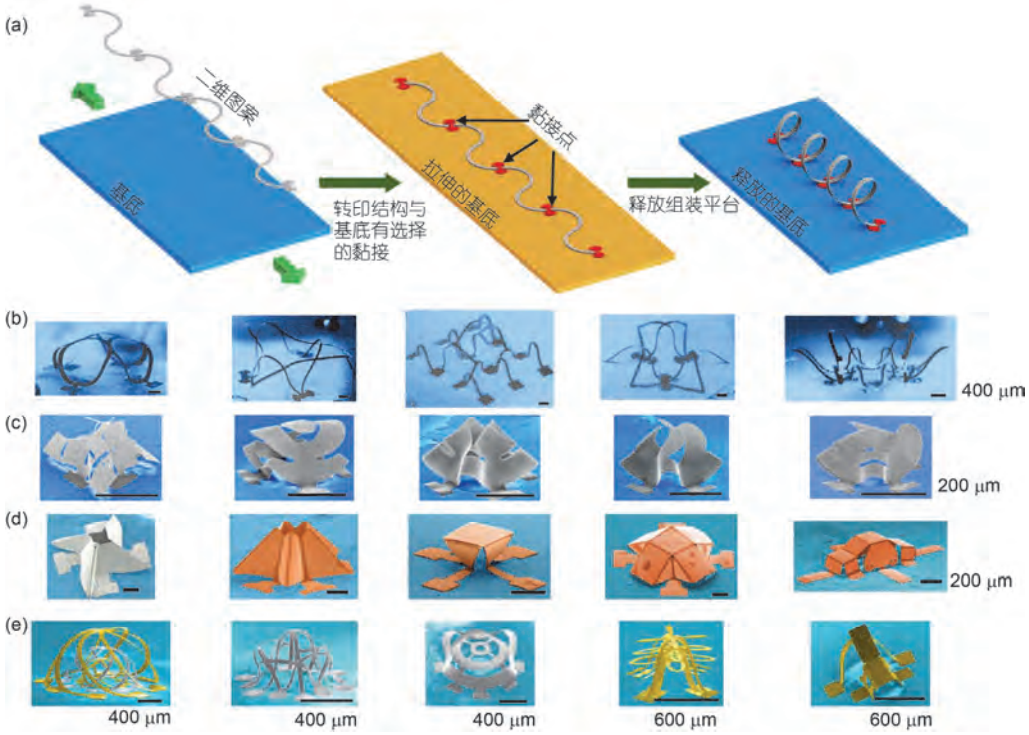

图 5 (网络版彩色)力学引导的组装方法示意图和典型结构. (a) 压缩屈曲引导组装的基本流程; (b) 三维条带状微结构[68]; (c) 引入剪纸设计的三维微结构[136]; (d) 引入折纸设计的三维微结构[137]; (e) 多层嵌套三维结构[67]

Figure 5 (Color online) Schemes of the mechanically guided self-assembly and some representative structures. (a) Schematic illustration of compressive buckling-guided assembly; (b) 3D filamentary mesostructures[68]; (c) 3D kirigami mesostructures[136]; (d) 3D origami mesostructures[137]; (e) 3D multilayer mesostructures[67]

结构[68]. 将剪纸和折纸概念引入初始二维结构的设计中, 可以实现更多种类的三维微结构[136,137,139]: 通过在初始二维结构中预设一些剪纸切口, 可以很大程度地减少由于局部扭结引起的应力集中, 并得到复杂的曲面状三维构型[136](图5(c)); 由于薄膜的弯曲刚度与厚度的立方成正比, 通过设计局部厚度减小,

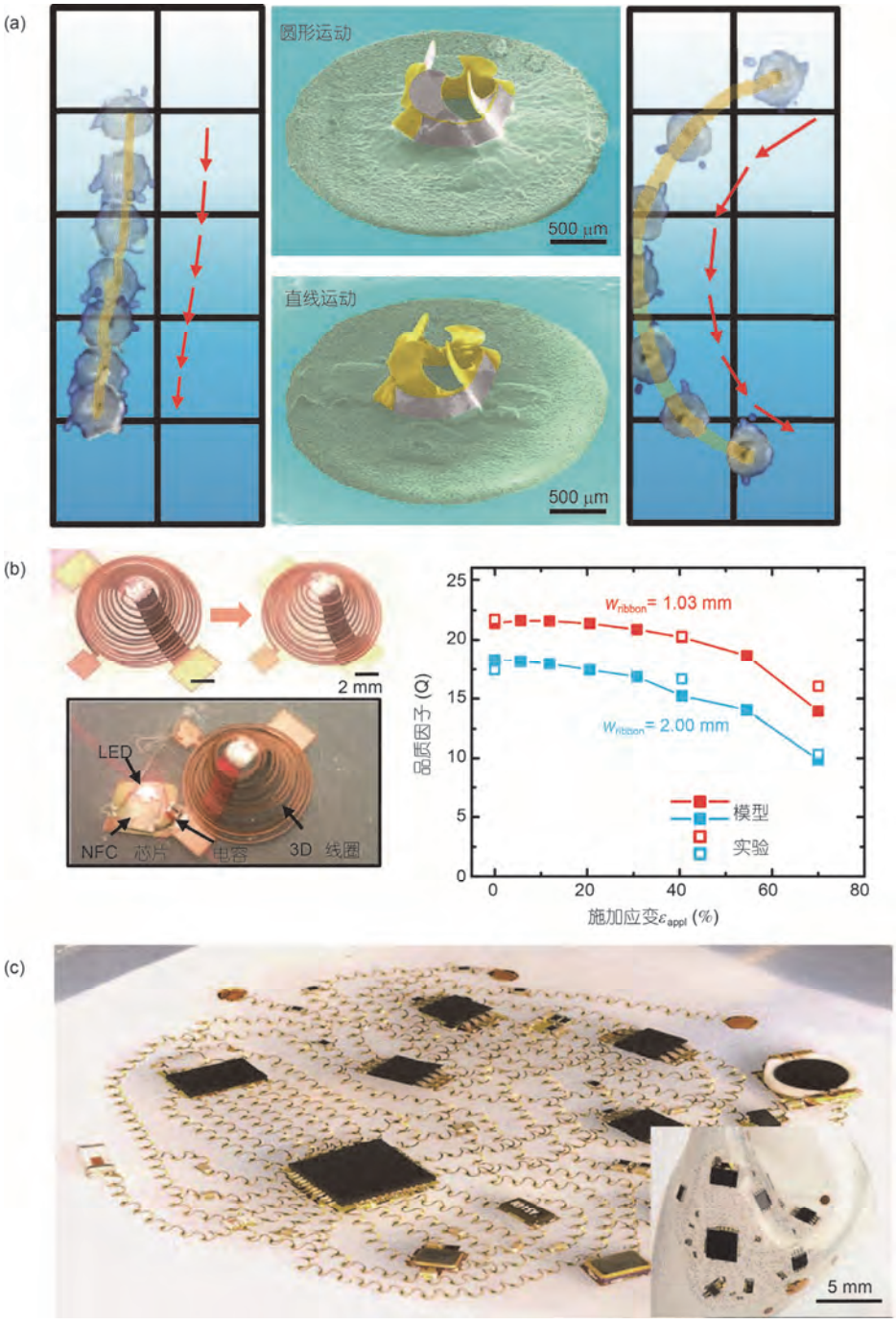

图 6 (网络版彩色)力学引导组装得到的三维细微观结构的应用. (a) 具有不同运动模式和轨迹的微型机器人[142]; (b) 近场通讯器件, 图中展示了两种不同条带宽度的器件的品质因子与加载应变的依赖关系[67]; (c) 基于三维螺旋型电导线的柔性电子器件[143]

Figure 6 (Color online) Applications of mesostructures assembled by mechanically guided method. (a) Microswimmers with controlled motion modes and trajectories[142]; (b) a 3D near-field communication device, with the graph illustrating the relationship between the Q factor and the applied strain for devices with two different ribbon widths[67]; (c) three-dimensional helical wires for stretchable electronics[143]

可以有效控制初始二维结构在指定位置发生折叠变形，实现结构的折纸设计[137](图5(d))．利用具有多层嵌套布局的初始二维设计，还可以得到空间利用率较高的密集型三维结构[67](图5(e))．此外，通过对弹性体基底进行几何和材料设计，可以让基底在预拉伸状态下实现特定的应变分布，进而更加精细地控制初始二维结构的屈曲变形[140]．

本方法的优势之一是其适用材料类型非常广泛，包括无机半导体、金属、聚合物以及各种不同的材料组合，并且其制备所得三维结构的尺度范围较广(从亚微米到米)[141]．由于力学引导的组装方法与传统平面加工工艺相兼容，因此可以将几乎任意类型的平面微系统转变为相应的三维微系统，从而为工程设计提供了更加广泛的选择，并有望制备得到具有新特性的微器件：如图6(a)所示，利用不同的独立三维结构，可以制备出有不同运动轨迹的微型机器人[142]；在图6(b)中，相对于传统二维结构，具有三维构型的近场通讯器件具有更高的品质因子，并能提供更大的有效工作角度[67]；在图6(c)中，将三维线圈应用于柔性电子的连接导线，能极大地增加整体器件的延展率[143]．此外，通过改变弹性软基底的释放路径，调整初始二维结构的加载方式，还可以实现可重构的三维微结构，为更多新型的微器件(如可隐身微型天线)提供设计方案[144]．

本方法的核心科学问题是薄膜结构(包括薄板和薄梁/条带结构)的后屈曲力学行为．由于薄板的大变形控制方程非线性太强，很难解析求解，通常利用有限元等数值计算工具进行求解．对于薄梁/条带结构

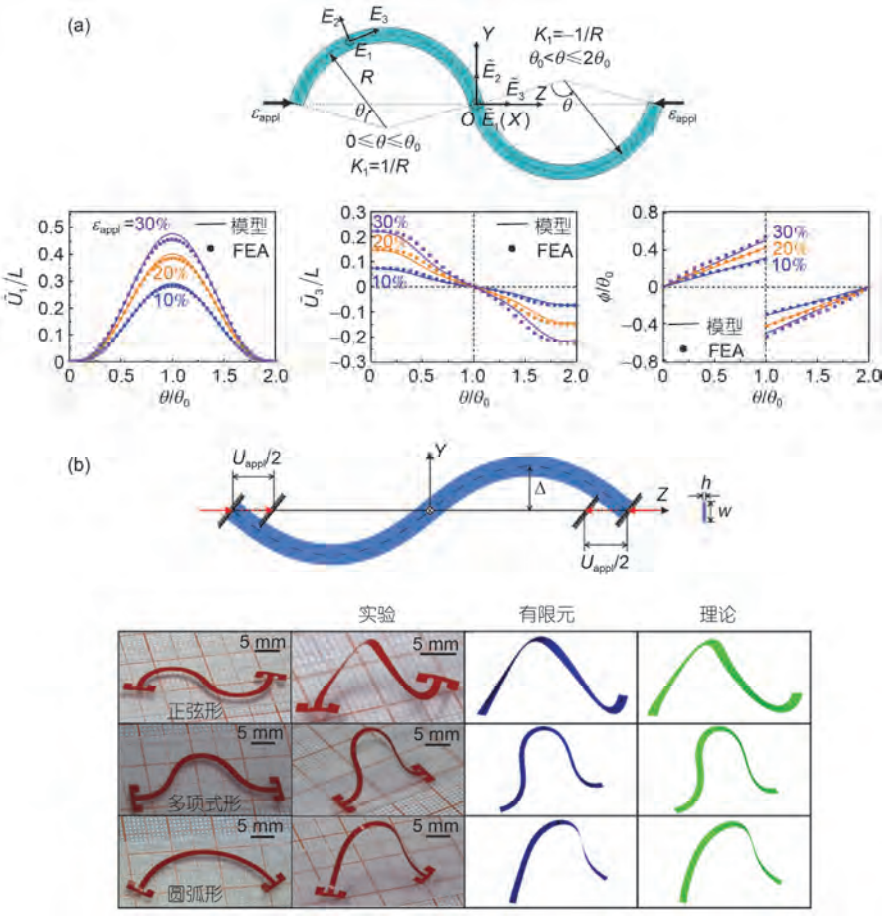

图 7　(网络版彩色)薄梁/条带后屈曲的理论模型．(a) 利用能量方法求解蛇形导线的弯扭失稳后屈曲问题[138]；(b) 采用摄动方法得到一般形式平面曲梁的后屈曲渐进解析解，图中展示了 3 种典型平面曲梁后屈曲的实验结果、有限元结果和理论结果，结构的加载应变为 30%[145]

Figure 7　(Color online) Theoretical models for the postbuckling of ribbons. (a) The lateral torsional postbuckling analysis of serpentine interconnects using an energetic method[138]; (b) asymptotic solutions for the postbuckling of general planar curved beams using a perturbation method, and the results for the postbuckling of three typical planar curved beams with an applied strain of 30%, based on experiment, FEA (Finite elemen analysis) and theoretical modeling[145]

的后屈曲行为, 近期在理论求解方面取得了一些新进展: 在图7(a)中, 对于微电子器件中常见的蛇形导线进行了理论分析, 利用能量最小原理, 求解了在不同初始几何参数下, 结构的弯扭失稳后屈曲问题[138]; 在图7(b)中, 研究对象为具有一般几何形式的平面条带, 通过采用摄动方法, 将非线性的平衡方程线性化, 建立了求解一般曲梁后屈曲行为的理论框架, 并得到了三种典型平面曲梁(正弦形、多项式形和圆弧形)的弯扭失稳后屈曲行为, 与有限元和实验结果对比良好, 相关结果可以用于三维条带结构的反向设计中[145].

在未来, 还需要进一步发展新的方法和工艺, 使得本方法可以推广到纳米尺度先进材料(如石墨烯等)的三维组装中.

3 讨论和结论

三维细微观结构在光电子器件、能量存储、生医器件等众多前沿领域都有着重要的应用前景, 因此发展针对三维细微观结构的新设计概念和制备方法显得十分必要. 近期的研究进展为三维细微观结构的制备提供了多种选择方案, 所得到的复杂三维构型十分繁多, 部分结构的关键特征尺寸甚至可达数十纳米或更小, 而结构整体尺寸可达厘米量级或更大. 本文中概述的各种方法都有其独特优势, 但同时各自也有一些局限性, 如: 4D打印方法可以实现非常复杂的三维图案, 但是对于材料类型有严格的限制, 且组装效率还有待提高; 基于微纳折纸的组装方法可以制备具有纳米特征尺寸的三维结构, 但其能得到的三维结构多为管状或多面体状, 几何拓扑范围很有限; 力学引导的组装方法可以有效克服前述方法中的不足, 但是由三维构型反推回初始二维几何设计的反问题模型还有待进一步研究发展. 将上述方法综合起来, 可为三维细微观结构的折叠与组装提供一套行之有效的解决方案. 除此之外, 从其他途径发展三维细微观结构的制备工艺也值得探索.

参考文献

1 Shelby R A, Smith D R, Schultz S. Experimental verification of a negative index of refraction. Science, 2001, 292: 77–79
2 Pendry J B, Holden A J, Robbins D J, et al. Magnetism from conductors and enhanced nonlinear phenomena. IEEE Trans Microwave Theory Tech, 1999, 47: 2075–2084
3 Smith D R, Pendry J B, Wiltshire M C K. Metamaterials and negative refractive index. Science, 2004, 305: 788–792
4 Smith D R, Padilla W J, Vier D C, et al. Composite medium with simultaneously negative permeability and permittivity. Phys Rev Lett, 2000, 84: 4184–4187
5 Pendry J B, Holden A J, Stewart W J, et al. Extremely low frequency plasmons in metallic mesostructures. Phys Rev Lett, 1996, 76: 4773–4776
6 Shelby R A, Smith D R, Nemat-Nasser S C, et al. Microwave transmission through a two-dimensional, isotropic, left-handed metamaterial. Appl Phys Lett, 2001, 78: 489–491
7 Schurig D, Mock J J, Justice B J, et al. Metamaterial electromagnetic cloak at microwave frequencies. Science, 2006, 314: 977–980
8 Parazzoli C G, Greegor R B, Li K, et al. Experimental verification and simulation of negative index of refraction using Snell's law. Phys Rev Lett, 2003, 90: 107401
9 Yen T J, Padilla W J, Fang N, et al. Terahertz magnetic response from artificial materials. Science, 2004, 303: 1494–1496
10 Linden S, Enkrich C, Wegener M, et al. Magnetic response of metamaterials at 100 terahertz. Science, 2004, 306: 1351–1353
11 Chen H T, Padilla W J, Zide J M O, et al. Active terahertz metamaterial devices. Nature, 2006, 444: 597–600
12 Zhang S, Fan W J, Panoiu N C, et al. Experimental demonstration of near-infrared negative-index metamaterials. Phys Rev Lett, 2005, 95: 137404
13 Valentine J, Zhang S, Zentgraf T, et al. Three-dimensional optical metamaterial with a negative refractive index. Nature, 2008, 455: 376–379
14 Liu N, Guo H C, Fu L W, et al. Three-dimensional photonic metamaterials at optical frequencies. Nat Mater, 2008, 7: 31–37
15 Lezec H J, Dionne J A, Atwater H A. Negative refraction at visible frequencies. Science, 2007, 316: 430–432
16 Cai W S, Chettiar U K, Kildishev A V, et al. Optical cloaking with metamaterials. Nat Photonics, 2007, 1: 224–227
17 Norris D J, Arlinghaus E G, Meng L L, et al. Opaline photonic crystals: How does self-assembly work? Adv Mater, 2004, 16: 1393–1399
18 Maldovan M, Thomas E L. Diamond-structured photonic crystals. Nat Mater, 2004, 3: 593–600
19 Jeon S, Park J U, Cirelli R, et al. Fabricating complex three-dimensional nanostructures with high-resolution conformable phase masks. Proc Natl Acad Sci USA, 2004, 101: 12428–12433

20 Jang J H, Ullal C K, Maldovan M, et al. 3D micro- and nanostructures via interference lithography. Adv Funct Mater, 2007, 17: 3027–3041
21 Campbell M, Sharp D N, Harrison M T, et al. Fabrication of photonic crystals for the visible spectrum by holographic lithography. Nature, 2000, 404: 53–56
22 Shir D, Nelson E C, Chen Y C, et al. Three dimensional silicon photonic crystals fabricated by two photon phase mask lithography. Appl Phys Lett, 2009, 94: 011101
23 Qi M H, Lidorikis E, Rakich P T, et al. A three-dimensional optical photonic crystal with designed point defects. Nature, 2004, 429: 538–542
24 Noda S, Tomoda K, Yamamoto N, et al. Full three-dimensional photonic bandgap crystals at near-infrared wavelengths. Science, 2000, 289: 604–606
25 Lin S Y, Fleming J G, Hetherington D L, et al. A three-dimensional photonic crystal operating at infrared wavelengths. Nature, 1998, 394: 251–253
26 LaFratta C N, Fourkas J T, Baldacchini T, et al. Multiphoton fabrication. Angew Chem Int Ed, 2007, 46: 6238–6258
27 Kawata S, Sun H B, Tanaka T, et al. Finer features for functional microdevices: Micromachines can be created with higher resolution using two-photon absorption. Nature, 2001, 412: 697–698
28 Deubel M, Von Freymann G, Wegener M, et al. Direct laser writing of three-dimensional photonic-crystal templates for telecommunications. Nat Mater, 2004, 3: 444–447
29 Cumpston B H, Ananthavel S P, Barlow S, et al. Two-photon polymerization initiators for three-dimensional optical data storage and microfabrication. Nature, 1999, 398: 51–54
30 Xu H Y, Shi X H, Gao F, et al. Ultrathin three-dimensional thermal cloak. Phys Rev Lett, 2014, 112: 054301
31 Narayana S, Sato Y. Heat flux manipulation with engineered thermal materials. Phys Rev Lett, 2012, 108: 214303
32 Han T C, Bai X, Gao D L, et al. Experimental demonstration of a bilayer thermal cloak. Phys Rev Lett, 2014, 112: 054302
33 Liu Z Y, Zhang X X, Mao Y W, et al. Locally resonant sonic materials. Science, 2000, 289: 1734–1736
34 Hussein M I, Leamy M J, Ruzzene M. Dynamics of phononic materials and structures: Historical origins, recent progress, and future outlook. Appl Mech Rev, 2014, 66: 040802
35 Fang N, Xi D J, Xu J Y, et al. Ultrasonic metamaterials with negative modulus. Nat Mater, 2006, 5: 452–456
36 Cummer S A, Christensen J, Alu A. Controlling sound with acoustic metamaterials. Nat Rev Mater, 2016, 1: 16001
37 Zheng X Y, Lee H, Weisgraber T H, et al. Ultralight, ultrastiff mechanical metamaterials. Science, 2014, 344: 1373–1377
38 Zheng X, Smith W, Jackson J, et al. Multiscale metallic metamaterials. Nat Mater, 2016, 15: 1100–1106
39 Silverberg J L, Evans A A, McLeod L, et al. Using origami design principles to fold reprogrammable mechanical metamaterials. Science, 2014, 345: 647–650
40 Schaedler T A, Jacobsen A J, Torrents A, et al. Ultralight metallic microlattices. Science, 2011, 334: 962–965
41 Overvelde J T, Weaver J C, Hoberman C, et al. Rational design of reconfigurable prismatic architected materials. Nature, 2017, 541: 347–352
42 Meza L R, Das S, Greer J R. Strong, lightweight, and recoverable three-dimensional ceramic nanolattices. Science, 2014, 345: 1322–1326
43 Jang D, Meza L R, Greer F, et al. Fabrication and deformation of three-dimensional hollow ceramic nanostructures. Nat Mater, 2013, 12: 893–898
44 Coulais C, Teomy E, de Reus K, et al. Combinatorial design of textured mechanical metamaterials. Nature, 2016, 535: 529–532
45 Babaee S, Shim J, Weaver J C, et al. 3D soft metamaterials with negative poisson's ratio. Adv Mater, 2013, 25: 5044–5049
46 Wang Q, Jackson J A, Ge Q, et al. Lightweight mechanical metamaterials with tunable negative thermal expansion. Phys Rev Lett, 2016, 117: 175901
47 Raffy S, Mascaro B, Brunet T, et al. A soft 3D acoustic metafluid with dual-band negative refractive index. Adv Mater, 2016, 28: 1760–1764
48 Brunet T, Merlin A, Mascaro B, et al. Soft 3D acoustic metamaterial with negative index. Nat Mater, 2015, 14: 384–388
49 Brunet T, Leng J, Mondain-Monval O. Soft acoustic metamaterials. Science, 2013, 342: 323–324
50 Yu M R, Huang Y, Ballweg J, et al. Semiconductor nanomembrane tubes: Three-dimensional confinement for controlled neurite outgrowth. ACS Nano, 2011, 5: 2447–2457
51 Tian B Z, Liu J, Dvir T, et al. Macroporous nanowire nanoelectronic scaffolds for synthetic tissues. Nat Mater, 2012, 11: 986–994
52 Leong T G, Randall C L, Benson B R, et al. Tetherless thermobiochemically actuated microgrippers. Proc Natl Acad Sci USA, 2009, 106: 703–708

53 Froeter P, Huang Y, Cangellaris O V, et al. Toward intelligent synthetic neural circuits: Directing and accelerating neuron cell growth by self-rolled-up silicon nitride microtube array. ACS Nano, 2014, 8: 11108–11117
54 Feiner R, Engel L, Fleischer S, et al. Engineered hybrid cardiac patches with multifunctional electronics for online monitoring and regulation of tissue function. Nat Mater, 2016, 15: 679–685
55 Wood R J. The challenge of manufacturing between macro and micro. Am Sci, 2014, 102: 124–131
56 Piyawattanametha W, Patterson P R, Hah D, et al. Surface- and bulk- micromachined two-dimensional scanner driven by angular vertical comb actuators. J Microelectromech Syst, 2005, 14: 1329–1338
57 Bishop D, Pardo F, Bolle C, et al. Silicon micro-machines for fun and profit. J Low Temp Phys, 2012, 169: 386–399
58 Zhang H G, Yu X D, Braun P V. Three-dimensional bicontinuous ultrafast-charge and -discharge bulk battery electrodes. Nat Nanotechnol, 2011, 6: 277–281
59 Wu H, Yu G, Pan L, et al. Stable Li-ion battery anodes by in-situ polymerization of conducting hydrogel to conformally coat silicon nanoparticles. Nat Commun, 2013, 4: 1943
60 Sun K, Wei T S, Ahn B Y, et al. 3D printing of interdigitated Li-ion microbattery architectures. Adv Mater, 2013, 25: 4539–4543
61 Pikul J H, Zhang H G, Cho J, et al. High-power lithium ion microbatteries from interdigitated three-dimensional bicontinuous nanoporous electrodes. Nat Commun, 2013, 4: 1732
62 Pan L, Yu G, Zhai D, et al. Hierarchical nanostructured conducting polymer hydrogel with high electrochemical activity. Proc Natl Acad Sci USA, 2012, 109: 9287–9292
63 Deng J W, Ji H X, Yan C L, et al. Naturally rolled-up C/Si/C trilayer nanomembranes as stable anodes for lithium-ion batteries with remarkable cycling performance. Angew Chem Int Ed, 2013, 52: 2326–2330
64 Lamoureux A, Lee K, Shlian M, et al. Dynamic kirigami structures for integrated solar tracking. Nat Commun, 2015, 6: 8092
65 Fan Z, Razavi H, Do J W, et al. Three-dimensional nanopillar-array photovoltaics on low-cost and flexible substrates. Nat Mater, 2009, 8: 648–653
66 Yu X, Huang W, Li M Y, et al. Ultra-small, high-frequency, and substrate-immune microtube inductors transformed from 2D to 3D. Sci Rep, 2015, 5: 9661
67 Yan Z, Zhang F, Liu F, et al. Mechanical assembly of complex, 3D mesostructures from releasable multilayers of advanced materials. Sci Adv, 2016, 2: e1601014
68 Xu S, Yan Z, Jang K I, et al. Assembly of micro/nanomaterials into complex, three-dimensional architectures by compressive buckling. Science, 2015, 347: 154–159
69 Rogers J, Huang Y G, Schmidt O G, et al. Origami MEMS and NEMS. MRS Bull, 2016, 41: 123–129
70 Huang W, Yu X, Froeter P, et al. On-chip inductors with self-rolled-up SiN_x nanomembrane tubes: A novel design platform for extreme miniaturization. Nano Lett, 2012, 12: 6283–6288
71 Huang W, Koric S, Yu X, et al. Precision structural engineering of self-rolled-up 3D nanomembranes guided by transient quasi-static FEM modeling. Nano Lett, 2014, 14: 6293–6297
72 Grimm D, Bufon C C B, Deneke C, et al. Rolled-up nanomembranes as compact 3D architectures for field effect transistors and fluidic sensing applications. Nano Lett, 2013, 13: 213–218
73 Ahn B Y, Duoss E B, Motala M J, et al. Omnidirectional printing of flexible, stretchable, and spanning silver microelectrodes. Science, 2009, 323: 1590–1593
74 Tumbleston J R, Shirvanyants D, Ermoshkin N, et al. Continuous liquid interface production of 3D objects. Science, 2015, 347: 1349–1352
75 Skylar-Scott M A, Gunasekaran S, Lewis J A. Laser-assisted direct ink writing of planar and 3D metal architectures. Proc Natl Acad Sci USA, 2016, 113: 6137–6142
76 Parekh D P, Ladd C, Panich L, et al. 3D printing of liquid metals as fugitive inks for fabrication of 3D microfluidic channels. Lab Chip, 2016, 16: 1812–1820
77 Murphy S V, Atala A. 3D bioprinting of tissues and organs. Nat Biotechnol, 2014, 32: 773–785
78 Ladd C, So J H, Muth J, et al. 3D printing of free standing liquid metal microstructures. Adv Mater, 2013, 25: 5081–5085
79 Konga Y L, Guptab M K, Johnsonc B N, et al. 3D printed bionic nanodevices. Nano Today, 2016, 11: 330–350
80 Kong Y L, Tamargo I A, Kim H, et al. 3D printed quantum dot light-emitting diodes. Nano Lett, 2014, 14: 7017–7023
81 Janusziewicz R, Tumbleston J R, Quintanilla A L, et al. Layerless fabrication with continuous liquid interface production. Proc Natl Acad Sci USA, 2016, 113: 11703–11708
82 Dickey M D, Chiechi R C, Larsen R J, et al. Eutectic gallium-indium (EGaIn): A liquid metal alloy for the formation of stable structures in microchannels at room temperature. Adv Funct Mater, 2008, 18: 1097–1104

83 Adams J J, Duoss E B, Malkowski T F, et al. Conformal printing of electrically small antennas on three-dimensional surfaces. Adv Mater, 2011, 23: 1335–1340
84 Tibbits S. 4D printing: Multi-material shape change. Archit Design, 2014, 84: 116–121
85 Raviv D, Zhao W, McKnelly C, et al. Active printed materials for complex self-evolving deformations. Sci Rep, 2014, 4: 7422
86 Gladman A S, Matsumoto E A, Nuzzo R G, et al. Biomimetic 4D printing. Nat Mater, 2016, 15: 413–418
87 Wu J T, Yuan C, Ding Z, et al. Multi-shape active composites by 3D printing of digital shape memory polymers. Sci Rep, 2016, 6: 24224
88 Ge Q, Qi H J, Dunn M L. Active materials by four-dimension printing. Appl Phys Lett, 2013, 103: 131901
89 Ge Q, Dunn C K, Qi H J, et al. Active origami by 4D printing. Smart Mater Struct, 2014, 23: 094007
90 Liu Y, Genzer J, Dickey M D. "2D or not 2D": Shape-programming polymer sheets. Prog Polym Sci, 2016, 52: 79–106
91 Kang S H, Dickey M D. Patterning via self-organization and self-folding: Beyond conventional lithography. MRS Bull, 2016, 41: 93–96
92 Huang G, Mei Y. Thinning and shaping solid films into functional and integrative nanomembranes. Adv Mater, 2012, 24: 2517–2546
93 Chen Z, Huang G, Trase I, et al. Mechanical self-assembly of a strain-engineered flexible layer: Wrinkling, rolling, and twisting. Phys Rev Appl, 2016, 5: 017001
94 Syms R R, Yeatman E M, Bright V M, et al. Surface tension-powered self-assembly of microstructures-the state-of-the-art. J Microelectromech Syst, 2003, 12: 387–417
95 Syms R R. Equilibrium of hinged and hingeless structures rotated using surface tension forces. J Microelectromech Syst, 1995, 4: 177–184
96 Syms R, Yeatman E. Self-assembly of three-dimensional microstructures using rotation by surface tension forces. Electron Lett, 1993, 29: 662–664
97 Pandey S, Ewing M, Kunas A, et al. Algorithmic design of self-folding polyhedra. Proc Natl Acad Sci USA, 2011, 108: 19885–19890
98 Gracias D H, Kavthekar V, Love J C, et al. Fabrication of micrometer-scale, patterned polyhedra by self-assembly. Adv Mater, 2002, 14: 235–238
99 Cho J H, Keung M D, Verellen N, et al. Nanoscale origami for 3D optics. Small, 2011, 7: 1943–1948
100 Py C, Reverdy P, Doppler L, et al. Capillary origami: Spontaneous wrapping of a droplet with an elastic sheet. Phys Rev Lett, 2007, 98: 156103
101 Guo X Y, Li H, Ahn B Y, et al. Two- and three-dimensional folding of thin film single-crystalline silicon for photovoltaic power applications. Proc Natl Acad Sci USA, 2009, 106: 20149–20154
102 Schmidt O G, Eberl K. Nanotechnology: Thin solid films roll up into nanotubes. Nature, 2001, 410: 168
103 Prinz V Y, Seleznev V A, Gutakovsky A K, et al. Free-standing and overgrown InGaAs/GaAs nanotubes, nanohelices and their arrays. Phys E, 2000, 6: 828–831
104 Li X L. Strain induced semiconductor nanotubes: From formation process to device applications. J Phys D Appl Phys, 2008, 41: 193001
105 Wang H, Zhen H, Li S, et al. Self-rolling and light-trapping in flexible quantum well-embedded nanomembranes for wide-angle infrared photodetectors. Sci Adv, 2016, 2: e1600027
106 Solovev A A, Mei Y, Bermúdez Ureña E, et al. Catalytic microtubular jet engines self-propelled by accumulated gas bubbles. Small, 2009, 5: 1688–1692
107 Prinz V Y, Seleznev V, Samoylov V, et al. Nanoscale engineering using controllable formation of ultra-thin cracks in heterostructures. Microelectron Eng, 1996, 30: 439–442
108 Mei Y F, Solovev A A, Sanchez S, et al. Rolled-up nanotech on polymers: from basic perception to self-propelled catalytic microengines. Chem Soc Rev, 2011, 40: 2109–2119
109 Mei Y, Huang G, Solovev A A, et al. Versatile approach for integrative and functionalized tubes by strain engineering of nanomembranes on polymers. Adv Mater, 2008, 20: 4085–4090
110 Malachowski K, Jamal M, Jin Q R, et al. Self-folding single cell grippers. Nano Lett, 2014, 14: 4164–4170
111 Karnaushenko D D, Karnaushenko D, Makarov D, et al. Compact helical antenna for smart implant applications. NPG Asia Mater, 2015, 7: e188
112 Bassik N, Stern G M, Jamal M, et al. Patterning thin film mechanical properties to drive assembly of complex 3D structures. Adv Mater, 2008, 20: 4760–4764
113 Bassik N, Stern G M, Gracias D H. Microassembly based on hands free origami with bidirectional curvature. Appl Phys Lett, 2009, 95: 091901
114 Wu Z L, Moshe M, Greener J, et al. Three-dimensional shape transformations of hydrogel sheets induced by small-scale modulation of internal stresses. Nat Commun, 2013, 4: 1586
115 Palleau E, Morales D, Dickey M D, et al. Reversible patterning and actuation of hydrogels by electrically assisted ionoprinting. Nat Commun, 2013, 4: 2257

116 Na J H, Evans A A, Bae J, et al. Programming reversibly self-folding origami with micropatterned photo-crosslinkable polymer trilayers. Adv Mater, 2015, 27: 79–85
117 Na J H, Bende N P, Bae J, et al. Grayscale gel lithography for programmed buckling of non-Euclidean hydrogel plates. Soft Matter, 2016, 12: 4985–4990
118 Klein Y, Efrati E, Sharon E. Shaping of elastic sheets by prescription of non-Euclidean metrics. Science, 2007, 315: 1116–1120
119 Kim J, Hanna J A, Byun M, et al. Designing responsive buckled surfaces by halftone gel lithography. Science, 2012, 335: 1201–1205
120 Liu Y, Boyles J K, Genzer J, et al. Self-folding of polymer sheets using local light absorption. Soft Matter, 2012, 8: 1764–1769
121 Hawkes E, An B, Benbernou N M, et al. Programmable matter by folding. Proc Natl Acad Sci USA, 2010, 107: 12441–12445
122 Felton S, Tolley M, Demaine E, et al. A method for building self-folding machines. Science, 2014, 345: 644–646
123 White T J, Broer D J. Programmable and adaptive mechanics with liquid crystal polymer networks and elastomers. Nat Mater, 2015, 14: 1087–1098
124 Ware T H, McConney M E, Wie J J, et al. Voxelated liquid crystal elastomers. Science, 2015, 347: 982–984
125 Ryu J, D'Amato M, Cui X, et al. Photo-origami—Bending and folding polymers with light. Appl Phys Lett, 2012, 100: 161908
126 Jamal M, Zarafshar A M, Gracias D H. Differentially photo-crosslinked polymers enable self-assembling microfluidics. Nat Commun, 2011, 2: 527
127 Yu X, Arbabi E, Goddard L L, et al. Monolithically integrated self-rolled-up microtube-based vertical coupler for three-dimensional photonic integration. Appl Phys Lett, 2015, 107: 031102
128 Blees M K, Barnard A W, Rose P A, et al. Graphene kirigami. Nature, 2015, 524: 204–207
129 Annett J, Cross G L. Self-assembly of graphene ribbons by spontaneous self-tearing and peeling from a substrate. Nature, 2016, 535: 271–275
130 Zhu S, Li T. Hydrogenation-assisted graphene origami and its application in programmable molecular mass uptake, storage, and release. ACS Nano, 2014, 8: 2864–2872
131 Zhu S, Li T. Hydrogenation enabled scrolling of graphene. J Phys D Appl Phys, 2013, 46: 075301
132 Qi Z N, Campbell D K, Park H S. Atomistic simulations of tension-induced large deformation and stretchability in graphene kirigami. Phys Rev B, 2014, 90: 245437
133 Patra N, Wang B, Král P. Nanodroplet activated and guided folding of graphene nanostructures. Nano Lett, 2009, 9: 3766–3771
134 Grosso B F, Mele E J. Bending rules in graphene kirigami. Phys Rev Lett, 2015, 115: 195501
135 Bahamon D A, Qi Z N, Park H S, et al. Graphene kirigami as a platform for stretchable and tunable quantum dot arrays. Phys Rev B, 2016, 93: 235408
136 Zhang Y H, Yan Z, Nan K W, et al. A mechanically driven form of Kirigami as a route to 3D mesostructures in micro/nanomembranes. Proc Natl Acad Sci USA, 2015, 112: 11757–11764
137 Yan Z, Zhang F, Wang J C, et al. Controlled mechanical buckling for origami-inspired construction of 3D microstructures in advanced materials. Adv Funct Mater, 2016, 26: 2629–2639
138 Liu Y, Yan Z, Lin Q, et al. Guided formation of 3D helical mesostructures by mechanical buckling: Analytical modeling and experimental validation. Adv Funct Mater, 2016, 26: 2909–2918
139 Shi Y, Zhang F, Nan K, et al. Plasticity-induced origami for assembly of three dimensional metallic structures guided by compressive buckling. Extrem Mech Lett, 2017, 11: 105–110
140 Nan K, Luan H, Yan Z, et al. Engineered elastomer substrates for guided assembly of complex 3D mesostructures by spatially nonuniform compressive buckling. Adv Funct Mater, 2017, 27: 1604281
141 Yan Z, Han M, Yang Y, et al. Deterministic assembly of 3D mesostructures in advanced materials via compressive buckling: A short review of recent progress. Extrem Mech Lett, 2017, 11: 96–104
142 Yan Z, Han M, Shi Y, et al. Three-dimensional mesostructures as high-temperature growth templates, electronic cellular scaffolds, and self-propelled microrobots. Proc Natl Acad Sci USA, 2017, 114: E9455–E9464
143 Jang K I, Li K, Chung H U, et al. Self-assembled three dimensional network designs for soft electronics. Nat Commun, 2017, 8: 15894
144 Fu H, Nan K, Bai W, et al. Morphable 3D mesostructures and microelectronic devices by multistable buckling mechanics. Nat Mater, 2018, 17: 268–276
145 Fan Z, Hwang K C, Rogers J A, et al. A double perturbation method of postbuckling analysis in 2D curved beams for assembly of 3D ribbon-shaped structures. J Mech Phys Solids, 2018, 111: 215–238

Summary for "三维细微观结构的折叠和组装方法"

Folding and assembly methods for forming three-dimensional mesostructures

Zhichao Fan, Fan Zhang & Yihui Zhang*

Applied Mechanics Laboratory, Ministry of Education, Department of Engineering Mechanics, Tsinghua University, Beijing 100084, China
* Corresponding author, E-mail: yihuizhang@tsinghua.edu.cn

In recent years, there has been an increasing interest in three-dimensional (3D) mesostructures with feature sizes between tens of nanometres and hundreds of micrometres. By forming 3D mesoscale architectures in advanced materials, the resulting materials systems are capable of offering novel acoustic, optical, thermal, mechanical and electronic properties that are not available in natural world, and are, thereby, also known as metamaterials. Owing to the tremendous application prospects of metamaterials in various advanced areas (e.g., electronics, photonics and energy storage), the design and the fabrication of 3D mesostructures has attracted growing attentions. In addition to the various techniques of 3D printing, another two classes of strategies have been developed, including the stress-controlled folding method and the mechanically guided assembly method.

In the context of stress-controlled folding method, advanced techniques such as 4D printing and micro-/nano-scale origami were proposed. As for the 4D printing, the planar structures formed by 3D printing techniques have a bilayer or multilayer heterogeneous architecture, in which mismatched strains resulted from external stimulation (e.g., heating) lead to 2D-to-3D transformation through self-folding or self-rolling. As for the micro-/nano-scale origami, the folding deformations are typically resulted from the forces induced by capillarity, thin-film residual stresses or mechanical stimuli response of active materials (for example, hydrogels, shape-memory polymers and shape-memory alloys).

In the mechanically guided assembly method, a strategically designed thin 2D precursor is fabricated by modern planar technologies (e.g., photolithography) and then transfer-printed onto a prestretched elastomer substrate. Then strong sites of adhesion are created between the 2D precursor and the substrate by selective bonding. Release of the prestretched substrate gives rise to compressive forces at the bonding areas, thereby transforming the 2D precursor into a 3D configuration by compressive buckling. The key design parameters of this method include: the geometric pattern, thicknesses and mechanical properties of the 2D precursor; the position of selective bonding; and the magnitude of the prestrain in the elastomeric substrate.

These two methods provide additional, unique options for the manufacturing of 3D mesostructures. The stress-controlled folding method usually applies to a limited class of 3D geometries, such as simple curved shells (e.g., tubes and scrolls), polyhedra and cylindrical structures. In comparison, the mechanically guided assembly method provides a route to more complex 3D topologies, because of the coupled translational and rotational deformations that can be controlled during the compressive buckling.

In this review, we summarize the latest progress of these two methods, and introduce the basic design principles and fabrication techniques. The resulting mesostructures with representative topologies are illustrated, along with the relevant design method and applications. Opportunities exist in the development of an integrated approach to combine effectively these existing methods, which might facilitate progress towards the goal of establishing methods that allow for rapid formation of arbitrary 3D architectures in any constituent materials.

3D assembly, 4D printing, 3D mesostructures, compressive buckling

doi: 10.1360/N972018-00396